Rationally Manipulating Aptamer Binding Affinities in a Stem-loop Molecular Beacon

Rachel E. Armstrong and Geoffrey F. Strouse*

Department of Chemistry and Biochemistry
Molecular Biophysics Program
Florida State University
Tallahassee, FL 32306-4390

Supporting Information

I. AuNP synthesis and NSET aptamer beacon characterization

A. AuNP synthesis. Spherical, 3nm AuNPs were synthesized using a modification of a published procedure, wherein $NaBH_4$ reduction of an aqueous solution of $HAuCl_4$ is carried out in the presence of thioctic acid (TA). The reaction produces water soluble, spherical AuNPs passivated by dihydrolipoic acid (DHLA) with a size of 3.0 ± 0.5 nm as evidenced by TEM distribution analysis. The TA is reduced by sodium borohydride to DHLA resulting in formation of two Au-S bonds to the free thiols on DHLA. The AuNPs were washed several times with nanopure H_2O and passed through a through a Millipore 10kDa centrifuge filter.

B . The Beer Lambert Law. The DNA distribution per AuNP was calculated from the UV-Vis spectra using the Beer Lambert Law, allowing the concentration of DNA and Au to be expressed in terms of the absorption intensity at 260 nm

$$A(total)_{260\ nm} = A(Au)_{260\ nm} + A(DNA)_{260\ nm}$$

$$= \{\varepsilon(Au)_{260}[Au] + \varepsilon\ (DNA)_{260}[DNA]\}b.$$

and at 520nm

$$A(total)_{520\ nm} = A(Au)_{520\ nm} = \{\ \varepsilon\ (Au)_{520}\ [Au]\ \}b$$

where A is the absorption value, ε is the extinction coefficient for the components and *b* is the pathlength of the cuvette (*b* = 1 cm). Solving for the AuNP concentration at 520nm allows the DNA concentration to be calculated at 260 nm (and indirectly the FAM concentration since the ratio on the synthetic sequence is 1:1 FAM to DNA).

C. UV-Vis, TEM and gel electrophoresis.

SF1. Characterization of the NSET Beacon. UV-Vis absorption spectra of the FAM-labeled DNA aptamer hairpin sequence (i), 3 nm DHLA-AuNP (ii), and the constructed NSET beacon (iii). The inset images depict gel electrophoretic data of the DHLA-AuNP and the NSET beacon as well as TEM data of the final NSET beacon.

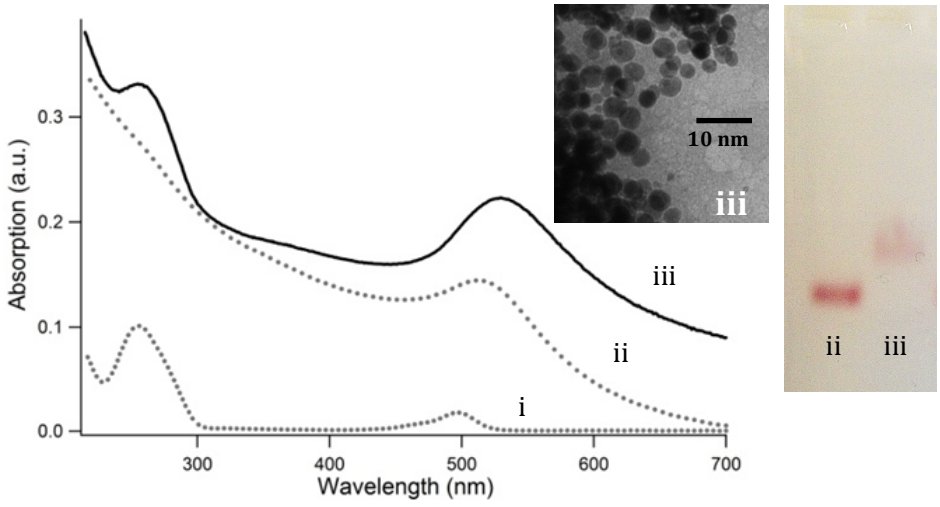

II. NSET efficiency and calculated distances

SF Table1. Table of NSET efficiencies and calculated AuNP-FAM distances. Using PL intensity measurements for FAM, NSET efficiencies at saturation (Imax) were calculated and the corresponding change in distance between the hairpin and ATP-bound states were calculated using NSET theory. The AuNP size dispersion value calculated by TEM is incorporated into the standard deviation of the FAM-AuNP distal values.

	I_0	FAM-AuNP distance at I_0 (Å)	I_{max}	FAM-AuNP distance at I_{max} (Å)
Seq *i*	0.19	77± 7	0.41± 0.05	101± 9
Seq *ii*	0.19	77± 7	0.38± 0.06	98± 10
Seq *iii*	0.19	77± 7	0.38± 0.05	98± 9
Seq *iv*	0.19	77± 7	0.44± 0.05	104± 9
Seq *v*	0.19	77± 7	1.0	----
Seq *vi*	0.61	124± 8	0.41± 0.06	101± 10

III. Control sequence *vi*

A. Sequence *vi* NSET aptamer beacon and saturation data.

SF2. Control sequence *vi*. Scheme depicting ATP binding to the non-hairpin control sequence *vi* and subsequent decrease in FAM intensity (A), sequence *vi* where the red, bold text represents the ATP aptamer sequence (B), and (1-ΔPL) versus [ATP] for sequence *vi* (C).

A)

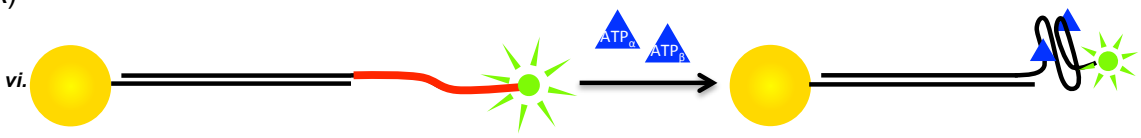

B)

Seq *vi*	5'(FAM) – CACTGT***CCTGGGGGAGTATTGCGGAGGAAGG***TTTTACAGTGGTGGAGGTGGAGGTG – 3' 3'- AAAATGTCACCACCTCCACCTCCAC – 5' NH_2

C)

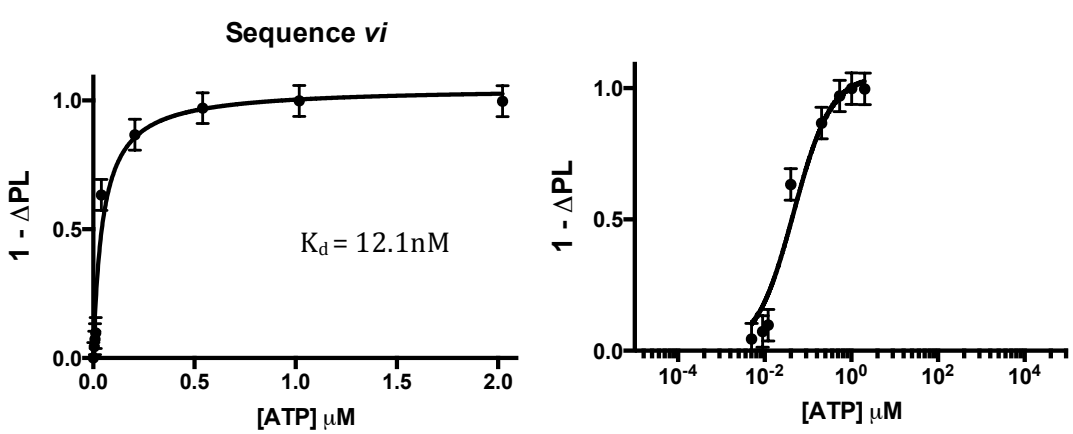

IV. Additional PL data

A. Change in PL with the addition of ATP.

SF3. Photoluminescent intensities of each stem-loop beacon with the addition of ATP. Selected concentrations of ATP are shown (with arrows) to indicate the magnitude and the direction of PL change. It should be noted that although initial concentrations of aptamer beacon were all ~1nM, inherent error in calculating beacon concentrations by UV-Vis absorption spectra cause the initial fluorescent intensities of the samples to be slightly unequal. The concentration and intensity measurements were measured against controls under identical conditions using 0 ATP and maximum saturation as the limiting values for each sequence measured. The reported intensities in the plot reflect the experimentally collected data, wherein concentrations, slit width, and averaging times were varied to allow the signal noise to be optimized for data collection. Therefore the intensities in the plots vary, but the quenching relative to control reported in the manuscript is corrected for the initial intensity variance.

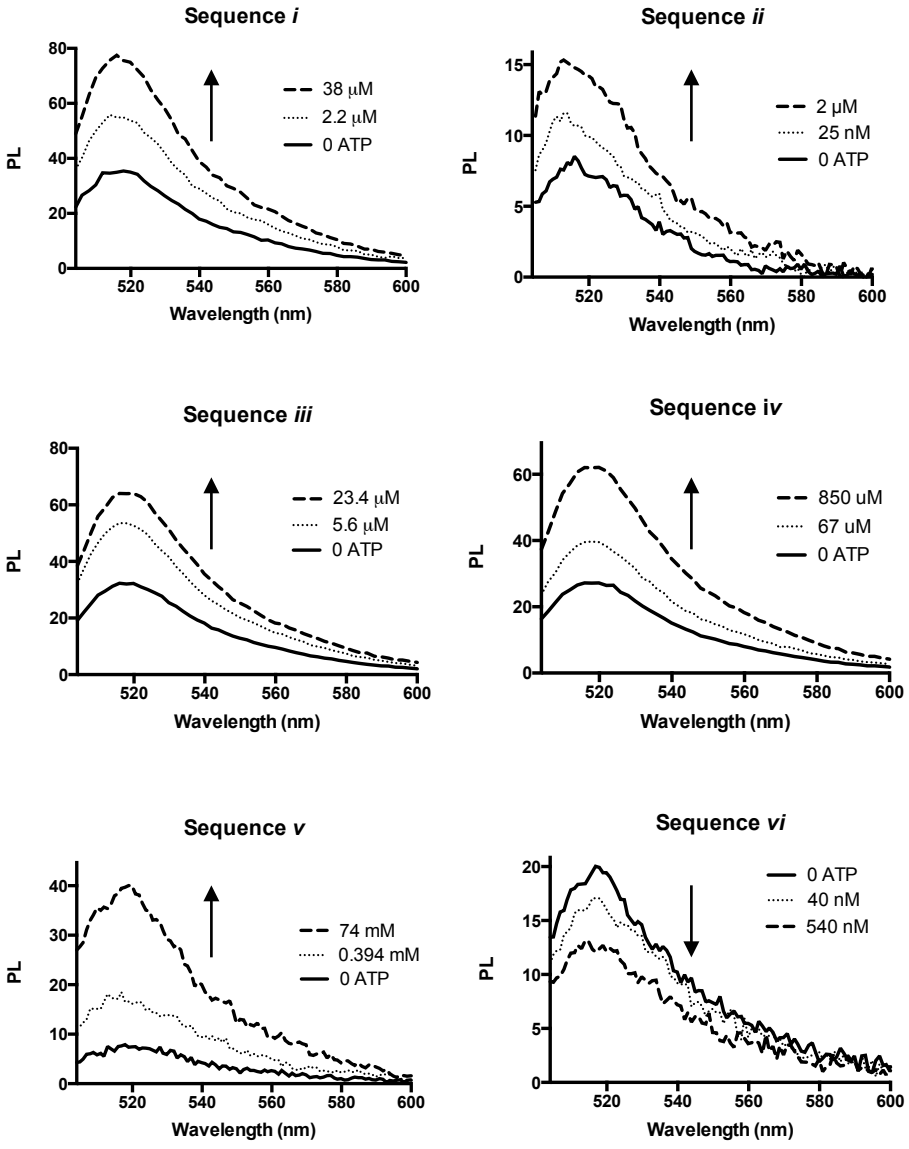

V. Statistical Analyses

A. Single-binding vs. two-binding event fits.

SF4. Saturation curves (Normalized PL $I\text{-}I_0$ vs. log[ATP]) were fit to a single-binding event model (A) and a two-binding event model (B) as described by the following equations:

$$(A)\ y = \left(\frac{B_{maxHi} * [ATP]}{K_{dHi} + [ATP]}\right) \qquad (B)\ y = \left(\frac{B_{maxHi} * [ATP]}{K_{dHi} + [ATP]}\right) + \left(\frac{B_{maxLo} * [ATP]}{K_{dLo} + [ATP]}\right)$$

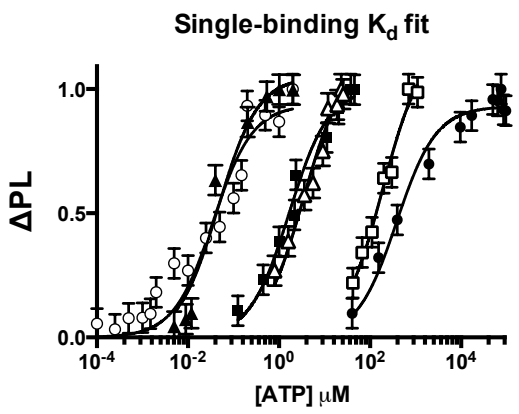

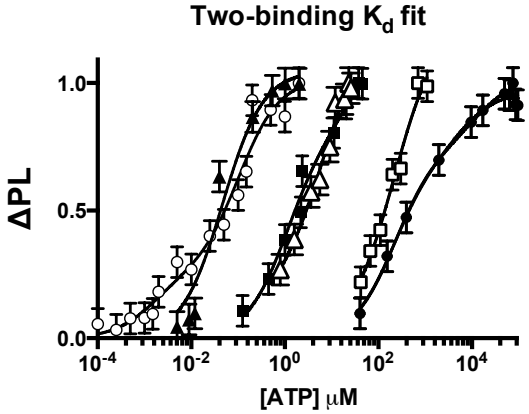

B. F test and Akaike's Test Values.

F test and Akaike's test (AIC) were employed to determine the statistical significance of the two-binding model vs. the single-binding model of ATP to its aptamer sequence. Both analyses evaluate the ratio of the sum of squares to the degrees of freedom when going from a simpler fit (single-binding model) to a more complex fit (two-binding model). Large values (>1) in the F test are indicative that the more complex fit is statistically significant, while a negative value in the AIC test is indicative of the more favorable complex fit. The equations for both test are below,

$$F = \left[\frac{\left(\frac{SS_1 - SS_2}{SS_2}\right)}{\left(\frac{DOF_1 - DOF_2}{DOF_2}\right)}\right] \qquad A = N\left(\ln\left[\frac{SS_2}{SS_1}\right]\right) + 2(DOF_1 - DOF_2)$$

where SS_1 and SS_2 are sum of squares for the single-binding and two-binding models, respectively, DOF_1 and DOF_2 are the degrees of freedom for the single-binding and two-binding models, respectively, and N is the number of points analyzed.

SF Table2. F test and AIC values. The F test and AIC value for each sequence analyzed in this study are listed in the table below.

	F test	***AIC***
Seq *i*	1.615	-0.307
Seq *ii*	8.754	-10.502
Seq *iii*	2.368	-1.818
Seq *iv*	1.498	-0.473
Seq *v*	7.940	-9.123
Seq *vi*	0	4

VI. Hill plots

A. Hill plots of the NSET aptamer beacons.

SF5. Hill plots of sequences *i-vi*, displayed below, are indicative of negative cooperatvitiy (*h*<1) in sequences *i-v* and extreme positive cooperativity in sequence *vi* (*h*>1).

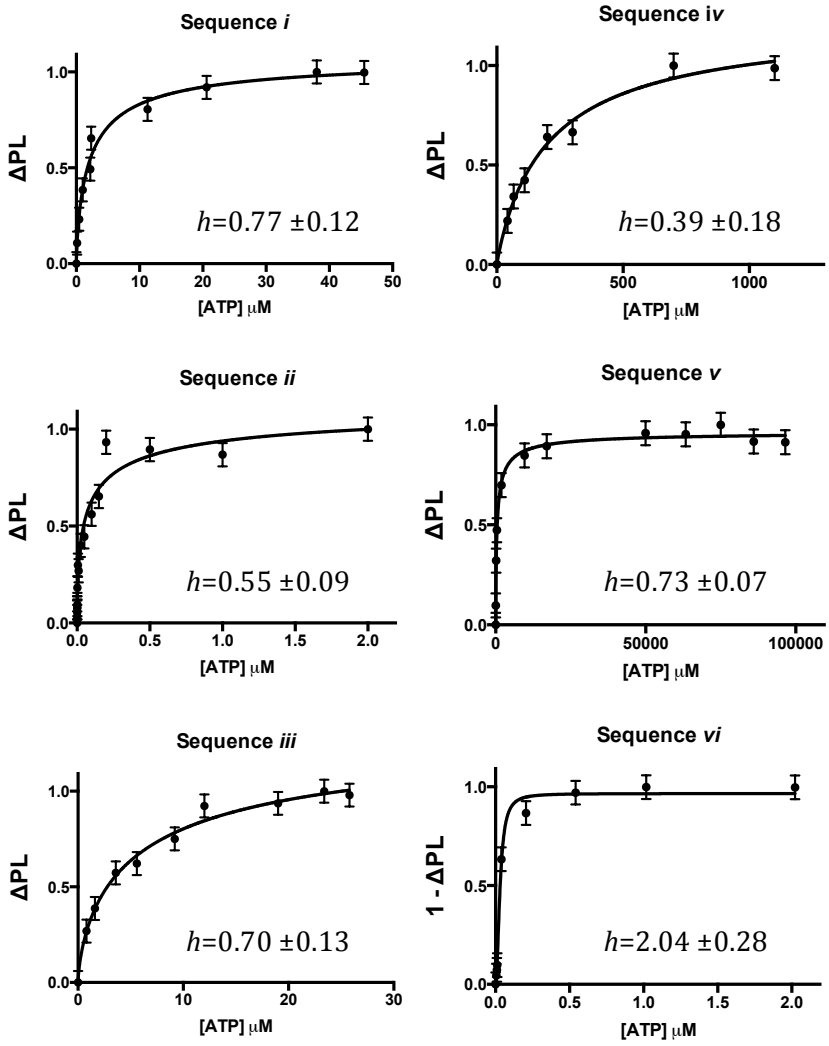

VII. Control studies

A. Effect of free AuNP on beacon response.

SF6. The effect of additional free AuNPs (2x NSET beacon concentration) on NSET aptamer beacon response is plotted below as a saturation curve (ΔPL vs. ATP concentration). The black circles represent the change in FAM intensity of a regular NSET aptamer beacon and the white triangles represent the change in FAM intensity of an NSET aptamer beacon in the presence of excess AuNPs, and demonstrates that free AuNPs do not impede ATP binding at the concentrations studied.

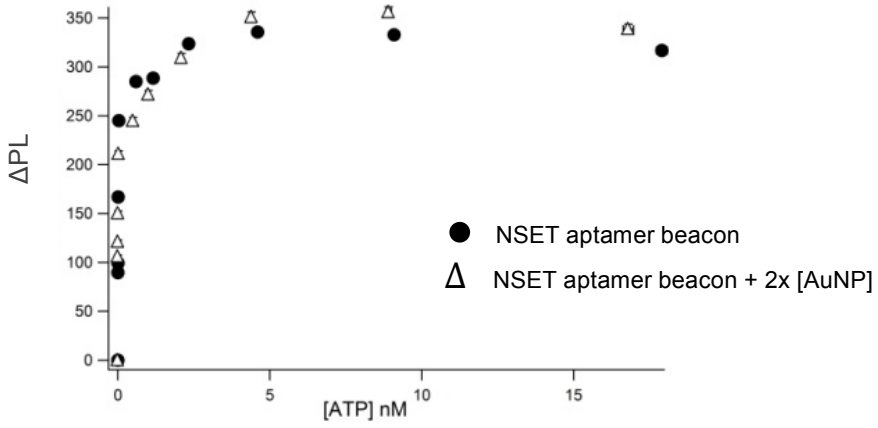

B. Specificity of the aptamer upon changes in duplex formation.

SF7. (a) To ensure changes in the aptamer's specificity are not contributing to the observed changes in binding affinity, similar studies using AMP were performed to monitor the scaling of the K_d between two of the sequences with different degrees of duplex formation (sequence *iii* and *iv*). Duplex formation adjustments between sequence *iii* and sequence *iv* in AMP studies result in K_d scaling similar to that observed in ATP studies, indicative of maintenance of selectivity of the aptamer amongst sequences.

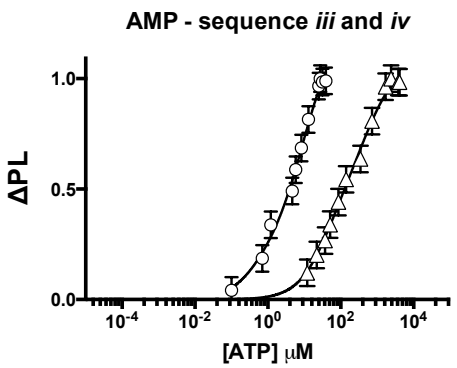

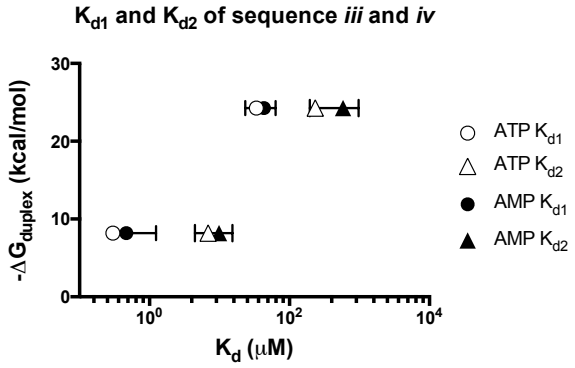

○ seq *iii* - K_{d1}, K_{d2} = 0.5 ± 0.7, 9.9 ± 5.4

△ seq *iv* - K_{d1}, K_{d2} = 43.3 ± 19.9, 584.0 ± 389.0

*Note: error bars shown for AMP values

(b) Sequence *ii*, sequence *iii*, and sequence *iv* were tested for their selectivity against two other nucleoside triphosphates UTP and GTP. As observed previously by other groups, this ATP DNA aptamer has no selectivity for non-adenosine phosphate molecules.

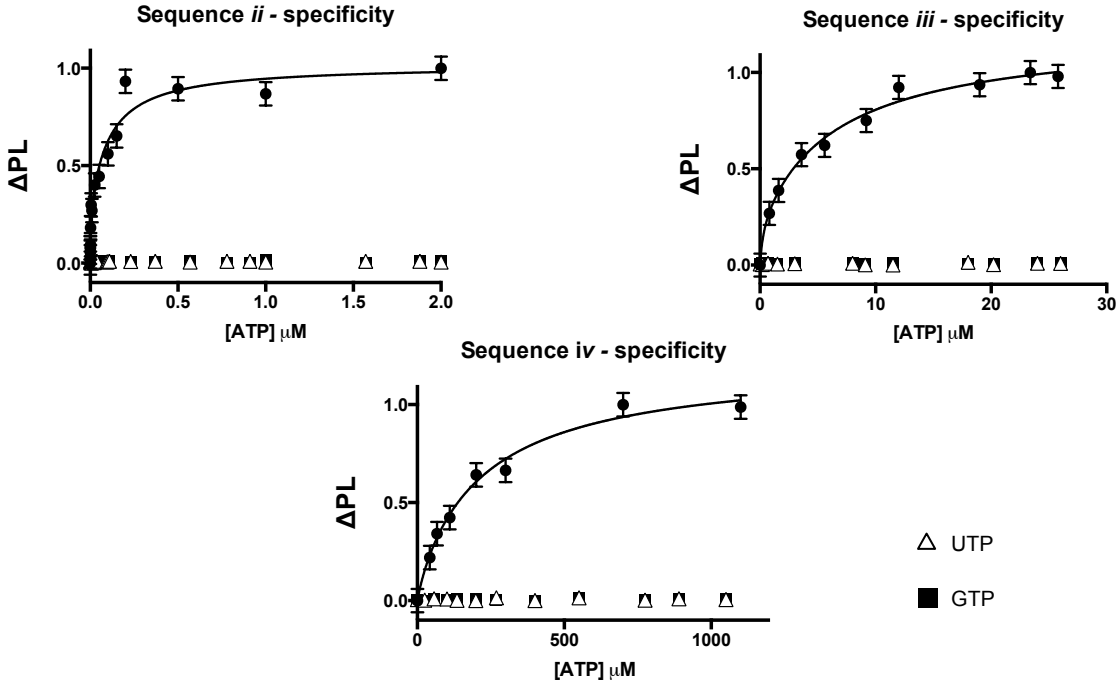

VIII. Nanometal Surface Energy Transfer.

SF8. A schematic depiction of NSET is shown below, where a fluorophore emission couples to the plasmon of the metal nanoparticle, followed by a release of energy in the form of heat from the metal nanoparticle:

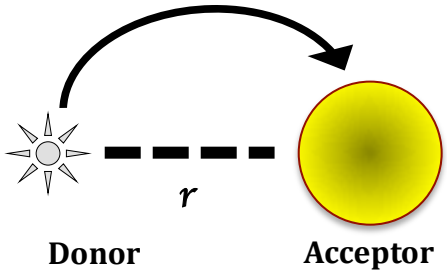

The NSET equation relating distance to energy transfer and the roles of the NSET donor (fluorescein) and acceptor (AuNP) are expressed in the following equation

$$d_0 = \frac{\alpha\lambda}{n_m}(A\Phi)^{1/4}\left[\frac{n_r}{2n_m}\left(\frac{1+\varepsilon_1^2}{\varepsilon_2^2}\right)\right]^{1/4}$$

where $\alpha = \frac{\left(\frac{9}{2}\right)^{1/4}}{4\pi}$ and $A = 10^3 ln10\left[\frac{\varepsilon_\lambda\left(2r_{cm}\left(\frac{2r_{cm}}{\gamma_{skin}}\right)\right)}{N_A V_{cm}^3}\right]$. The distance in which 50% energy transfer occurs is represented by d_0, λ is the emission wavelength of the fluorophore, n_m is the refractive index of the medium, n_r is the refractive index of the metal, Φ is the quantum yield of the fluorophore, ε_1 is the dielectric constant of the medium, and ε_2 is the dielectric constant of the metal. In the subsequent equations, N_A is avogadro's number, ε_λ is the dielectric constant as a function of λ, r_{cm} is the radius of the AuNP in centimeters, γ_{skin} is the skin depth of the AuNP, and V_{cm} is the volume of the AuNP in cm^3.

Calculating $R_{0<avg>}$ from the particle distribution convoluted with the NSET expression. The calculated R_0 from the NSET expression is based upon a single AuNP size. Experimentally the size is represented as a new Gaussian distribution obtained by TEM size analysis. The distribution function can be incorporated into the NSET expression yielding a $R_{0<avg>}$ value that incorporates the perturbation arising from the measured size distribution. A plot of the effective quenching calculated between fluorescein and a 3 ± 0.5 nm AuNP for the weighted Gaussian distribution from the FWHM value attained from the TEM images shown below.